Heliyon 5 (2019) e02553

Contents lists available at ScienceDirect

Heliyon

journal homepage: www.heliyon.com

Heliyon

Research article

Adsorption kinetic and thermodynamic studies of the 2, 4 – dichlorophenoxyacetate (2,4-D) by the [Co–Al–Cl] layered double hydroxide

Josiane S. Calisto, Ingrid S. Pacheco, Leonardo L. Freitas, Laiane K. Santana, Wélique S. Fagundes, Fábio A. Amaral, Sheila C. Canobre *

LAETE - Laboratório de Armazenamento de Energia e Tratamento de Efluentes, Institute of Chemistry, UFU- Uberlândia Federal University, João Naves de Ávila Avenue, 2121, 38400-902, Uberlândia- Minas Gerais, Brazil

ARTICLE INFO

Keywords:
Inorganic chemistry
Environmental science
Layered double hydroxides
Adsorption
Herbicide
dichlorophenoxyacetate

ABSTRACT

[Co–Al–Cl] layered double hydroxide (LDH) obtained by co-precipitation at constant pH 8 presented a single phase in a hexagonal unit cell parameters similar to the hydrotalcite (JCPDS 14-191) belonging to the rhombohedral crystal system and space group $R_{(-3)m}$. The adsorption kinetics of 2,4-D onto [Co–Al–Cl] LDH was better described by the Pseudo Second-Order (best adjust $R^2 = 0.9998$ for 60 mg L^{-1} 2,4-D adsorption). Intra-particle diffusion model was not the sole rate-controlling factor, indicating the adsorption of 2,4-D by the [Co–Al–Cl] LDH is a complex process for the experimental conditions performed, involving both boundary layer and intra-particle diffusion. The adsorption isotherm adjusted better to the Freundlich model ($R^2 = 0.9845$) and the ΔH° value of - 51.18 kJ mol^{-1} indicated the predominance of the physical adsorption. The FT-IR spectrum of LDH after adsorption presented 2,4-D bands together with those of LDH and XRD showed an increase in the inter-lamellar distance (d_{003}) due to the intercalation of 2,4-D in the interlayer structure of the [Co–Al–Cl] LDH, corroborating inter and intra-particle adsorption data. Thus, [Co–Al–Cl] LDH, commonly used as electrodes in supercapacitors, can be effectively used as an adsorbent for the removal of 2,4-D from contaminated waters.

1. Introduction

The current concern with the widespread contamination of soils and groundwater from the application of pesticides in modern agriculture is driving the development of research into recovery and treatment alternative processes. In this context, adsorption is considered one of the most cheap and practical of purification and separate processes due versatility and accessibility in residual water treatment, allowing the hazardous compounds removal in wastewater. In addition, is one of the main physicochemical processes used for the removal of pesticides in soils and contaminated water (Haddad et al., 2019; Aumeier et al., 2019).

The search for low cost alternative materials for the removal of environmental pollutants has been growing in recent years. In this sense, clays have received special attention in the pesticides adsorption study (Khoei et al., 2019; Ye et al., 2019), pharmaceuticals (Ghemit et al., 2017), metals (Shujun et al., 2018; Khoei et al., 2019) and others substances considered caused environmental damage. In this sense, the search for low cost alternative materials for the removal of environmental pollutants has been growing in recent years. The Layered double hydroxide (LDH) has a basic structure formed by cationic layers, composed of divalent and trivalent cations hexacoordinated to hydroxyl ions in an octahedral arrangement (Crepaldi et al., 2000).

Synthetic compounds of the hydrotalcite type are similar to the structure of the mineral hydrotalcite, which in turn has layers with structures of the brucite $Mg(OH)_2$ type. The general formula $[M^{2+}_{1-x}M^{3+}_{x}(OH)_2]^{x+}A^{m-}_{x/m}.nH_2O$ describes the chemical composition of hydrotalcite-type compounds, where: M^{2+}(divalent metal cation), M^{3+} (anion charge), M^- (charge of the anion) and $X = M^{3+}/(M^{3+} + M^{2+})$ where X is the Molar ratio. Thus, from different metal ions (divalent and another trivalent) and interlayer species, LDH can be prepared by different methods such as: by coprecipitation at pH constant or variable, hydrolysis of the urea, sol-gel, or by regeneration of the calcined precursor (Crepaldi and Valim, 1998; Crepaldi et al., 2000). Thus, this material presents a variety of applications, such as: catalytic process (Bialas et al., 2016) electrochemical application as electrodes in batteries and supercapacitors (Lai et al., 2015) and adsorbents of pesticides (Pavlovic

* Corresponding author.
E-mail address: sheila.canobre@ufu.br (S.C. Canobre).

https://doi.org/10.1016/j.heliyon.2019.e02553
Received 2 March 2019; Received in revised form 12 August 2019; Accepted 27 September 2019

et al., 2013).

Among the herbicides, 2,4 – dichlorophenoxyacetate (2,4 - D) was the first successful selective herbicide, which quickly became the most widely used in the world. 2,4-D appears predominantly in its anionic form in the pH range that exists in the natural environment and it is highly mobile and poorly biodegradable (Carter, 2000). The half-life of 2, 4-D in water ranges from one to several weeks under aerobic conditions, and it can exceed 120 days under anaerobic conditions (WHO, 2003). 2, 4-D poses a high threat to surface and ground water supplies due to its high mobility and toxicity. Besides, it is among the priority contaminants of major environmental concern (Hamilton et al., 2003; WHO, 2003). Thus, there is a need for the development of an efficient and cost-effective adsorbent for removing 2,4-D from water (Feng et al., 2008). Removal of the 2,4 - D is commonly reported using [Cu–Fe–NO_3] LDH or [Mg–Zn–Al] LDH as adsorbent material (Nejati et al., 2013; Zhao et al., 2018; Zhang et al., 2018) or using other intercalation methodologies such as: anion exchange of a precursor LDH, direct synthesis by co-precipitation, rehydration of a calcined LDH precursor and thermal reaction (Newman and Jones, 1998). So, in this work, [Co–Al–Cl] LDH, commonly used as electrodes in supercapacitors (Pourfarzad et al., 2019; Gao et al., 2018; Li et al., 2017a,b; Qiu and Villemure, 1997), was synthesized by the co-precipitation method at constant pH and tested as adsorbent for the removal of 2,4-D from contaminated waters. The adsorption isotherms and the kinetic curves were also measured experimentally.

2. Materials and methods

2.1. Materials

[Co–Al–Cl] LDH were synthesized by coprecipitation method at constant pH 8, using 1.0 mol L^{-1} $CoCl_2.6H_2O$ (BIOTEC P.A.) and 0.5 mol L^{-1} $AlCl_3.6H_2O$ (BIOTEC P.A.). A basic solution of 1.0 mol L^{-1} NaOH (VETEC P.A) was slowly added to control the pH.

The dosage of the 2,4-D (ALDRICH 98%) used were 40, 60 and 80 mg L^{-1} and masses of [Co–Al–Cl] LDH were 100 and 200 mg in adsorption tests.

2.2. Synthesis of [Co–Al–Cl] LDH by coprecipitation at constant pH

[Co–Al–Cl] LDH was synthesized by the coprecipitation method at constant pH (8.0 ± 0.5). For this, a solution of 500 mL containing 1.0 mol L^{-1} hexahydrate cobalt chloride - $CoCl_2.6H_2O$ and 0.5 mol L^{-1} nonahydrate aluminum chloride - AlCl3. $9H_2O$, with a ratio of 2: 1. A solution of 1.0 mol L^{-1} NaOH was added slowly to the mixture solution containing 1.0 mol L^{-1} $CoCl_2.6H_2O$ and 0.5 mol L^{-1} $AlCl_3.6H_2O$, aiming at the pH control equal to 8. The precipitate obtained was filtered, washed and then dried under vacuum at 60–80 °C for 48 h (Crepaldi et al., 2000).

2.3. Characterization of materials

2.3.1. Structural characterization of [Co–Al–Cl] LDH by XRD

The structural characterization was performed by X-ray diffraction (XRD) in a Shimadzu diffractometer (Model 6000, radiation Cu Kα, λ = 1.5406 Å) with a voltage of 40 kV, current of 30 mA, at 2θ min^{-1} from 5 to 70°. The unit cell parameters, a, c and d were calculated d was calculated using the Fullprof program. The d003-value corresponds to the sum of the thickness and height of the interlayer region.

2.3.2. Surface area characterization of [Co–Al–Cl] LDH by B.E.T

Specific surface area measurements were performed on a Micrometrics equipment, model ASAP 2020, by adsorption of N_2. The samples were pre-treated under vacuum at 90 °C for 4 h.

2.3.3. Microstructural characterization by fourier transform infrared (FT-IR)

FT-IR spectroscopy measurements were performed using an infrared spectrophotometer (FT-IR Frontier Single Range – MIR da Perkin Elmer) in the region between 4000 and 500 cm^{-1}. The measurements were made in solid state, using the Attenuated Total Reflectance (ATR) accessory with diamond crystal.

2.3.4. Determination of the pH of zero charge point (pH_{ZCP})

The pH_{ZCP} was determined for LDH, in order to check the pH range in which [Co–Al–Cl] LDH behave like cationic or anionic. The procedure for determining the pH_{ZCP} consisted of adding 1 g L^{-1} [Co–Al–Cl] LDH in 0.1 mol L^{-1} NaCl aqueous solution (increasing ionic strength) in different conditions of starting pH, from 2 to 12, (Regalbuto and Robles, 2004). The solutions were filtered and the final pH of the solution has been determined after 24 h of equilibration at 25 °C (Feigenbrugel et al., 2006). The pH_{ZCP} correspond to the range in which the final pH is kept constant regardless of the initial pH. The acid solutions were prepared from HCl 0.1 mol L^{-1} dilutions and from the NaOH aqueous solution 0.1 mol L^{-1} dilutions.

2.4. Batch adsorption experiments of the 2,4-D by [Co–Al–Cl] LDH

2.4.1. Factorial experiment (2^3)

The optimization of parameters affecting the adsorption was performed using a two-level full factorial experimental design with a central point involving three factors: initial concentration of the 2,4-D (20 mg L^{-1} (-1) and 100 mg L^{-1}(+1)), [Co–Al–Cl] LDH adsorbent mass (100 mg (-1) and 200 mg (+1)) and pH 3 (-1) and 5 (+1) at 25 °C, 200 rpm and 60 min of equilibration time. The supernatants were recovered to measure the residual concentration of the herbicide which was determined by UV-Vis spectroscopy. The absorbance was measured at 230 nm (Feigenbrugel et al., 2006) in a Shimadzu UV-1650DC (UV-Visible Spectrophotometer). The experimental data were processed using the Statistica® software, the performance factors and the interactions between them were evaluated on the results obtained by the Pareto graph. To obtain adsorption capacity values (q), a mass balance is carried out, in which the amount of adsorbate in the adsorbent must be equal to the amount of adsorbate removed from the solution, or, in mathematical terms (Eq. 1) (Kinniburgh, 1986).

$$qt = \frac{V\,(Co - Ce)}{m} \tag{1}$$

where C_o (mg L^{-1}) is the initial concentration of 2,4-D, C_e (mg L^{-1}) is the 2,4-D concentration at time t (min), m (g) is the mass of adsorbent LDH, V (L) is the volume of adsorbate solution and q_t (mg g^{-1}) is the adsorbed amount at time t (min).

2.4.2. Determination of equilibration time and adsorption kinetics

50 mL of 2,4-D solution at different concentrations (40; 60 and 80 mg L^{-1}) at pH 5 received a mass of 150 mg of [Co–Al–Cl] LDH in erlenmeyers. At room temperature 298 K under 200 rpm shaking until the collection time previously set at 10, 20, 30, 40, 60, 90, 120, 150, 180 and 240 min. Then, each collected sample aliquot was measured in a UV-Vis at the maximum wavelength of 230 nm. To investigate the adsorption kinetics of 2,4-D onto LDH, used linear models, denoted Pseudo-First-Order, Pseudo- Second-Order, Intraparticle and Film Diffusion models.

2.4.3. Determination of adsorption isotherms

50 mL of 2,4-D solution at different concentrations (40; 60 and 80 mg L^{-1}) at pH 5 were maintained in contact with 150 mg of [Co–Al–Cl] LDH under agitation of 200 rpm for 60 min. The experiment was carried out at

4 temperatures (298, 308, 318 and 328 K). Adsorption isotherms were adjusted using the Langmuir and Freundlich models in linearized forms.

2.4.4. Effect of temperature on adsorption thermodynamic parameters

The thermodynamic parameters were estimated from the data of isotherms de Freundlich, since they were exposed to four different temperatures (298, 308, 318 and 328 K). Thermodynamic parameters can evaluate the orientation and feasibility of the adsorptive reaction. The three thermodynamic parameters considered were in Gibbs free energy (ΔG^o), standard enthalpy (ΔH^o) and standard entropy (ΔS^o).

3. Results and discussion

3.1. Structural characterization of [Co–Al–Cl] LDH

Fig. 1 (a) show the X-ray diffractogram for [Co–Al–Cl] LDH synthesized at pH constant 8. It was observed diffraction peaks at $2\theta = 22.72°$, 44.43° and 60.12°, corresponding to the reflections 006, 018 and 110, respectively, can being indexed to the layered structure, consistent with the JCPDS No. 14-191, concerning the hydrotalcite. Inorganic layers of LDH resulted in a hexagonal unit cell belonging to the rhombohedral crystal system and space group $R_{(-3)m}$. Besides, it was realized the Rietveld refinement for this [Co–Al–Cl] LDH. The experimental points (in red), the calculated curve (in black) and the difference between them (in green) are represented in the XRD pattern. The vertical bars indicate the positions of the *Bragg* reflections for each crystalline phase, noting the presence of the single-phase hydrotalcite type.

Then, to evaluate the quality of the refined structural model, it was calculated R_{Bragg} and X^2, which showed values of 1.61 and 1.73, respectively (Table 1).

3.2. Specific surface area characterization of [Co–Al–Cl] LDH by B.E.T

The pore classification of [Co–Al–Cl] LDH was mesopores considering that the average diameter of the pores and average width of the pores is between 2 nm < *diameter* < 50 nm (Gregg and Sing, 1982). The specific surface area and pore volume values for [Co–Al–Cl] LDH were 43.48 $m^2 g^{-1}$ and 0.048 $cm^3 g^{-1}$, respectively. These values are coherent with those obtained by Mostafa and Mohamed (2016) and Bernardo et al. (2016).

3.3. Determination of the pH of zero charge point (pH_{ZCP})

In order to prescribe the pH range wherein the adsorbent [Co–Al–Cl] LDH possessed a cationic character which would favor the adsorption with herbicide that has a negative charge density 2,4-D. The pH of zero charge point of [Co–Al–Cl] LDH was determined between the pHs 2 and 12. In Fig. 2 is shown the final pH after 24 h of adsorption as a function of pH prior to adsorption.

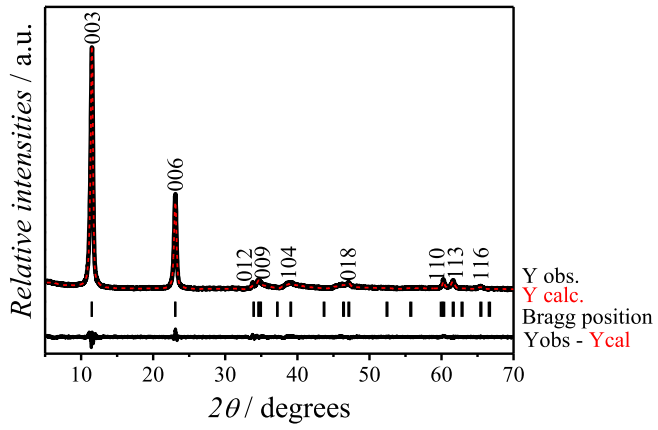

Fig. 1. Rietveld refinement of the [Co–Al–Cl] LDH synthesized by coprecipitation at constant pH 8.

Table 1
Crystallographic parameters obtained from the Rietveld fitting of the XRD data.

[Co–Al–Cl] LDH Parameter			Indicator
R_B	1.61	-	R – Bragg
R_F	3.48	-	R – Structure Factor
R_{wp}	5.07	-	R – Pondered profile
R_{exp}	3.85	-	R-Expected
S	1.32	~1	Set Quality
χ^2	1.73	<2	Refinement Quality

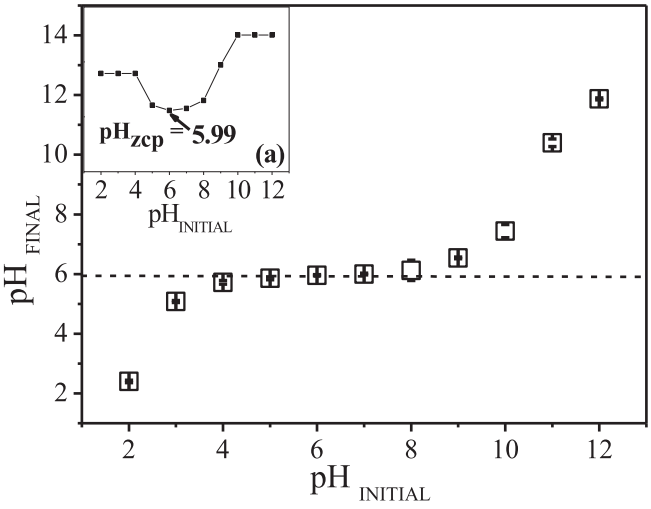

Fig. 2. Variation of initial pH as a function of final pH (zero charge point) of the [Co–Al–Cl] LDH synthesized by coprecipitation at constant pH 8.

The pH_{ZCP} was calculated from the arithmetic average of the final pH.The [Co–Al–Cl] LDH synthesized at pH constant 8 showed a pH_{ZCP} value of 5.99. This specific pH range occurs with electroneutral charges on the surface of the adsorbent. At pH values below pH_{ZCP}, the surface active sites are protonated, presenting a surface with positive charge density. Thus, the herbicide adsorption process was conducted at pHs below 5.99, to enhance the electrostatic attraction between [Co–Al–Cl] LDH and 2,4-D (anionic herbicide).

3.4. Adsorption test of the 2,4-D by [Co–Al–Cl] LDH

3.4.1. Factorial experiment (2^3)

The treatment of the data obtained using analysis of variance (ANOVA) and statistical probability (p = 0.05) resulted in the Pareto graph shown in Fig. 3. The results show that adsorbent mass and 2,4-D concentration were effects more significant in the adsorption process. The adsorbent mass was the most significant factor, revealing a positive effect. Based on this observation, it can be inferred that when the ratio between sorbent and sorbate is high there are more active sites available, favoring the adsorption efficiency.

It is well known that the concentration of the 2,4-D solution is the main factor affecting the adsorption properties This variable showed a negative effect, indicating that an increase in the concentration value results in an decrease in the rate de 2,4-D adsorption due to saturation of the active sites of the adsorbent by the adsorbate molecules (Table 2).

Table 2 show the experimental matrix of the factorial design (2^3) and capacity adsorption of the herbicide 2,4-D by [Co–Al–Cl] LDH.

3.4.2. Determination of equilibration time and adsorption kinetics

The contact time indicates the kinetic behavior of the adsorption for a given adsorbent at a given initial adsorbate concentration. Fig. 4 shows the effect of the contact time for 2,4-D adsorption on [Co–Al–Cl] LDH at

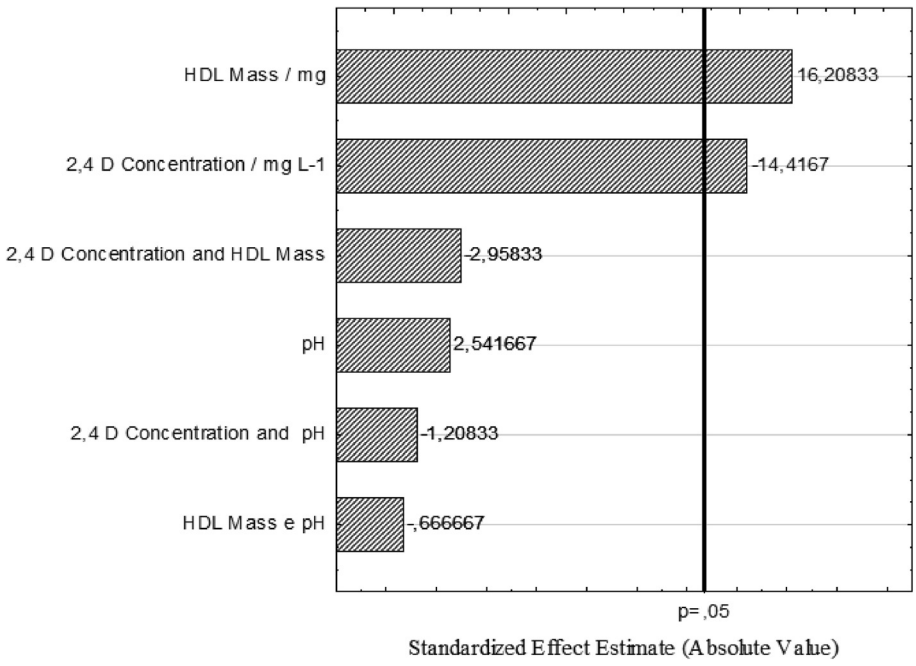

Fig. 3. Pareto graph for full factorial design.

Table 2
Experimental matrix of the factorial design (2^3) for the study of the adsorption of the herbicide 2,4-D by adsorbent [Co–Al–Cl] LDH.

Experiment	pH	[Co–Al–Cl] LDH mass/mg	2,4-D dosage/mg L^{-1}	Q Adsorption/mg g^{-1}	Adsorptionpercentage/%
1	3 (-1)	100 (-1)	20 (-1)	5.51	55.06
2	5 (+1)	100 (-1)	20 (-1)	6.33	63.29
3	3 (-1)	200 (+1)	20 (-1)	4.34	86.71
4	5 (+1)	200 (+1)	20 (-1)	4.50	89.87
5	3 (-1)	100 (-1)	100(+1)	20.51	41.01
6	5 (+1)	100 (-1)	100 (+1)	21.27	42.53
7	3 (-1)	200 (+1)	100 (+1)	15.16	60.63
8	5 (+1)	200 (+1)	100 (+1)	15.79	63.16

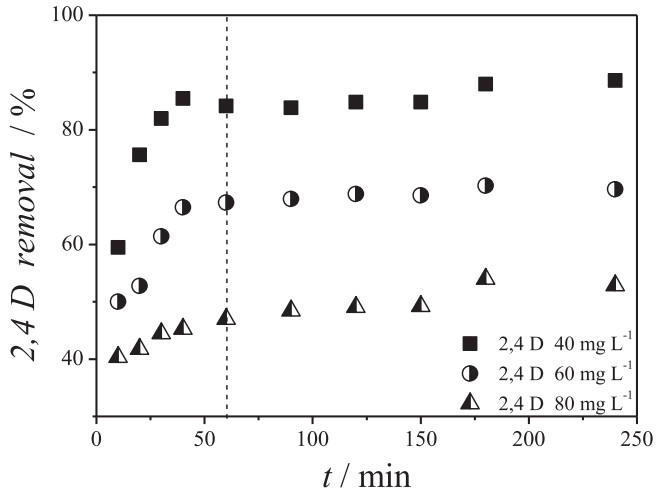

Fig. 4. Amount of 2,4-D as a function of time at different 2,4-D dosages.

pH = 5 as a function of different dosages of the adsorbent. The removal of 2,4-D increases rapidly during the initial 2,4-D adsorption stages due to sites available for sorption on the surface. However, with increasing surface coverage, the number of remaining binding sites decrease dowing to the repulsive forces between the adsorbed and free molecules, leading to the equilibrium state being achieved (Yu et al., 2017). The equilibrium state was achieved after 60 min, which was used for Kinetic and Thermodynamic studies.

Two kinetic models were considered (Fig. 5 (a) and (b)) Pseudo-First-Order and Pseudo-Second-Order) to investigate the mechanism of 2,4-D adsorption (Eq. 2 and Eq. 3, respectively). These models are the most commonly used to describe the adsorption of organic and inorganic pollutants onto solid adsorbents. Linear kinetic models were compared using the R^2 value as reference.

$$Ln(qe - qt) = lnln\, qe - k_1 t \tag{2}$$

$$\frac{1}{(q_e - q_t)} = \frac{1}{q_t} + k_2 t \tag{3}$$

where q_e and q_t are the amounts of 2,4-D adsorbed at equilibrium, in mg g^{-1}, and at time t, in min, respectively, k_1 and k_2 are the pseudo first order rate constant (min^{-1}) and second order rate constant (g mg^{-1} min^{-1}) respectively.

According to the linear fitted plots presented in Fig. 5 (a) and (b) and kinetic parameters, the adsorption kinetics of 2,4-D onto [Co–Al–Cl] LDH is better described by the Pseudo Second-Order kinetic model (R^2 0.9998 for 2,4-D 60 mg L^{-1} adsorption) than the Pseudo First-Order (R^2 0.4026 for 2,4-D 60 mg L^{-1} adsorption). The correlation coefficient for the pseudo-second-order model ($R^2 > 0.99$, Table 3), suggesting that the sorption process was mainly dominated by multiplex mechanisms involved in herbicide removal (Yu et al., 2018).

A plot that expresses the amount of adsorbate adsorbed, qt (mg g^{-1})

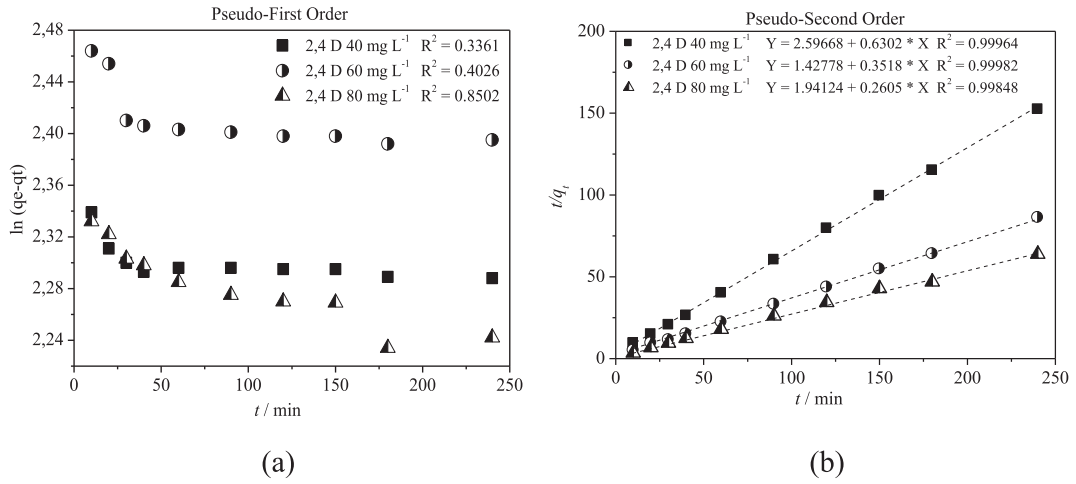

Fig. 5. Kinetic adsorption data: (a) Pseudo-First Order and (b) Pseudo-Second Order models for 2,4-D by the [Co–Al–Cl] LDH at different 2,4-D dosages.

Table 3
Kinetic parameters predicted by pseudo-first order, pseudo-second order and for adsorption of 2,4 D by [Co–Al–Cl] LDH.

2,4 D (mg L^{-1})	Pseudo First Order		Pseudo Second Order	
	K_1 (min^{-1}) * 10^4	R^2	K_2 (g mg^{-1} min^{-1}) * 10^2	R^2
40	1.2524	0.3361	15.2947	0.9996
60	2.2584	0.4026	8.6668	0.9998
80	3.8411	0.8502	3.4957	0.9985

as a function of the square root of the time, gives the rate constant by calculating the plot slope. This model can be described by Eq. (4) (Weber and Morris, 1963):

$$q_t = K_{id}\ \sqrt{t} + C \tag{4}$$

where k_{id} (mg g^{-1} $min^{-0.5}$) and C are diffusion coefficient and intra-particle diffusion constant, respectively. *C* is directly proportional to the thickness of the boundary layer.

According to Weber and Morris (1963) if intraparticle diffusion is the determinant of velocity, the removal of the adsorbate varies with the square root of time and passes through the origin. Fig. 6 (a) shows the plot of amount adsorbed of 2,4-D, q_t (mg g^{-1}), *versus* $t^{1/2}$. Film diffusion model (Fig. 6 (b) was also used to investigate if transport of 2,4-D from the liquid phase up to the solid phase boundary also plays a role in the adsorption process Eq. (5) (Boyd et al., 1947):

$$-\ln\left(1-\frac{q_t}{q_e}\right) = K_{fd}\ t \tag{5}$$

Where K_{fd} is the liquid film diffusion constant.

The plots (Fig. 6 (a) are nonlinear for the whole range of studied concentrations, indicating that intraparticle diffusion is not the only rate-limiting step, but other process may also be involved in the adsorption. The adsorption process is not a one-step process as evidenced by the curvature in these plots and two different sharp stages are clearly observed. The first stage, including the adsorption period from 0 to 40 min ($t^{1/2} < 6.3$), describes the instantaneous adsorption stage where 2,4-D adsorption rate is high due to low competition between the 2,4-D molecules. Intraparticle diffusion was not the predominant mechanism in the adsorption in the range up to 40 min ($t^{1/2} = 6.3$), since the first stage the linear coefficient was different of zero and the intraparticle diffusion constant (C) varied from 0.85 to 2.3 mg g^{-1}. The second stage, ranging from 40 to 240 min ($6.3 < t^{1/2}) < 15.5$), is attributed to the low adsorption stage caused by the low concentration gradients, producing the equilibrium condition. When diffusion equilibrium is reached in the second stage, the intra-particle diffusion slows down due to saturation of most of the adsorption sites and this is evidenced by the plateaus.

The adsorption process follows the film mechanism when the plots of ln ($1 - q_t/q_e$) *vs.* *t* at different adsorbent dosages are linear or non linear but do not pass through the origin, thereby explaining the influence of

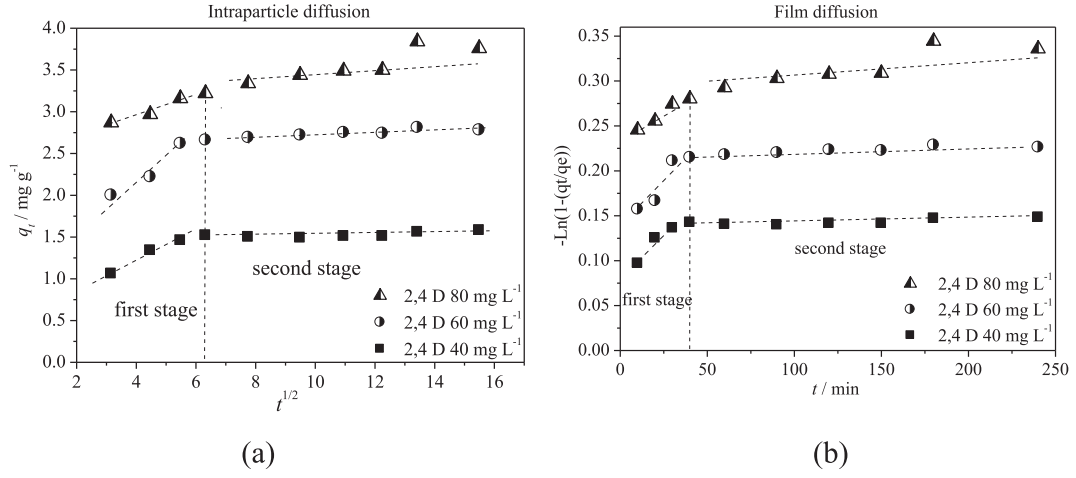

Fig. 6. (a) Intraparticle diffusion and (b) Film diffusion models for 2,4-D adsorption by the [Co–Al–Cl] LDH at different 2,4-D dosages.

Table 4
Kinetic parameters predicted by Intraparticle and film diffusion models for adsorption of 2,4 D by [Co–Al–Cl] LDH.

2,4 D (mg L^{-1})	Intraparticle Diffusion model		Film Diffusion model	
	K_{id} (mg g^{-1} $min^{-0,5}$) *10^2	R^2	K_{fd} (min^{-1}) *10^5	R^2
40	1.161	0.8910	5.150	0.9133
60	1.331	0.8674	5.210	0.8587
80	6.211	0.8855	2.730	0.8775

film diffusion mechanism on the adsorption rate. Likewise, by comparing the data presented in Table 4, the R^2 values for the intraparticle diffusion values were similar to those of the film diffusion model. These results suggest that both processes occur simultaneously during the 2,4-D adsorption process. Then, intra-particle diffusion model was not the sole rate-controlling factor, indicating the adsorption of 2,4-D by the [Co–Al–Cl] LDH is a complex process, involving both boundary layer and intra-particle diffusion.

The values of k_{id} and K_{fd} were determined from the slopes of the linear plots (second stage) and presented in Table 4.

3.5. Determination of adsorption isotherms

In order to establish the type of adsorption prevailing between the herbicide and [Co–Al–Cl] LDH, two types of isotherms were tested (Freundlich and Langmuir models).

To better understand the characteristics of the adsorption process, the equilibrium adsorption data were analyzed by well-known Langmuir (Eq. 6) and Freundlich (Eq. 7) linear models (Langmuir, 1918; Freundlich, 1906).

$$\frac{C_e}{q_e} = \frac{1}{q_{max}} * C_e + \frac{1}{k_L * q_{max}} \quad (6)$$

$$\ln(q_e) = \ln(k_f) + \frac{1}{n} * \ln(C_e) \quad (7)$$

where Ce (mg/L) is the equilibrium concentration of 2,4-D remained in the solution, qe (mg/g) is the amount 2,4-D adsorbed on per weight unit of solid after equilibrium, q_{max} (mg/g) is the maximum adsorption capacity, k_L is adsorbate/adsorbent interaction constant (L mg^{-1}); K_F is a measure of adsorvent capacity and the slope *1/n* is the adsorption intensity.

Fig. 7 (a) and (b) shows that adsorption isotherm adjusted to the Freundlich (R^2 = 0.9845) rather than Langmuir (R^2 = 0.9023), particularly at low concentrations and at 308 K (where was the best adjust), indicating the occurrence of physical and chemical and adsorptions, respectively. Thus, this adjustment preferably to the Freundlich model demonstrates the formation of multilayer interaction action between adsorbent and adsorbate.

Table 5 show parameters of both model adjusts in different temperatures. The q_{max} and K_L parameters obtained from Langmuir isotherm represent the maximum adsorption capacity and adsorbate/adsorbent interaction constant, respectively. Table 5 shows that the q_{max} value decreases with increasing temperature and the K_L increases, since the adsorption process of 2,4-D by [Co–Al–Cl] LDH is exothermic. The K_F and *1/n* represent the Freundlich constants, referring to the maximum adsorption capacity and adsorption intensity, respectively. The parameter *1/n* calculated from the Freundlich model is in the interval from 0 to 1, suggesting that the 2,4-D adsorption onto LDH is favorable and also that there are minimum interactions between the adsorbed molecules (Fytianos et al., 2000; Tsai et al., 2005). The K_F value decreases with increasing temperature, because this constant is related to the maximum adsorption capacity, which decreases with increasing temperature.

Table 6 shows that the adsorption capacity of the [Co–Al–Cl] LDH is consistent with that obtained for other materials tested as adsorbent for the removal of 2,4-D.

3.6. Effect of temperature on adsorption thermodynamic parameters

The effect of temperature of the 2,4–D adsorption on the [Co–Al–Cl] LDH was investigated under isothermal conditions in the temperature range 298–328 K. The 2,4-D adsorption capacity onto [Co–Al–Cl] LDH decreases with increasing temperature, suggesting that the adsorption reaction is exothermic. The change in standard free energy (ΔG°), enthalpy (ΔH°) and entropy (ΔS°) of adsorption were calculated using Eqs. (8) and (9). The Freundlich constant K_F can be obtained as a dimensionless value using Eq. (10) (Tran et al., 2016).

Table 5
Equilibrium parameters of Langmuir and Freundlich models of 2,4-D.

Model	Parameters	298 K	308 K	318 K	328 K
Langmuir	q_{max} (mg g^{-1})	30.120	27.174	25.974	23.364
	K_L (10^2.L mg^{-1})	0.9428	1.1240	1.2223	1.3895
	R^2	0.8785	0.9023	0.8494	0.6973
Freundlich	K_F ((10^1 mg g^{-1}) (L $mg^{-1})^{1/n}$)	8.536	8.146	5.969	5.532
	1/n	0.603	0.627	0.719	0.704
	R^2	0.9722	0.9845	0.9689	0.9837

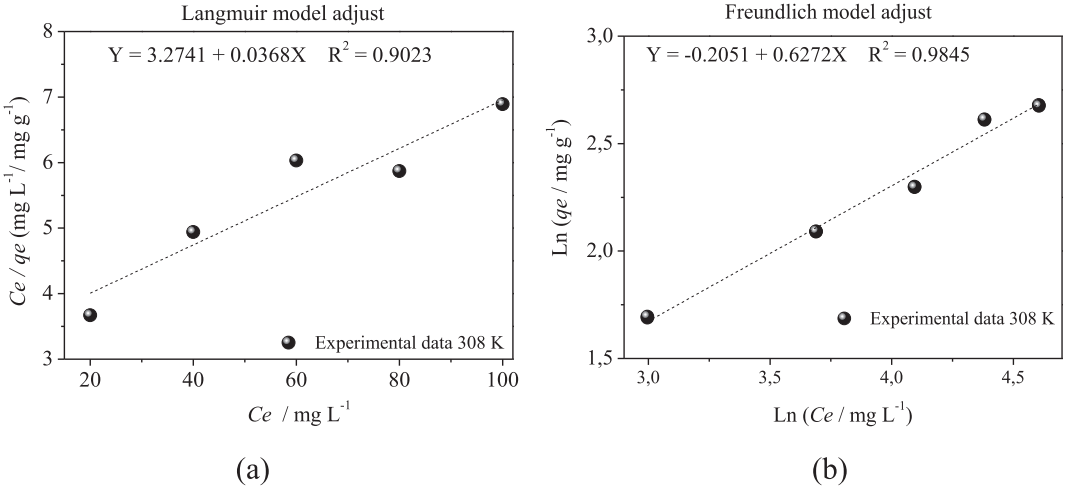

Fig. 7. (a) Langmuir adjust and (b) Freundlich adjust models for 2,4-D adsorption by the [Co–Al–Cl] LDH at 308 K.

Table 6
Comparison of 2,4-D adsorption of this work and previous studies.

Adsorbent	Adsorption capacity, q_m (mg g^{-1})	Reference
Commercial AC (F-300)	181.82	(Salman and Hameed, 2010)
Chitin	6.07	(El Harmoudi et al., 2014)
Chitosan	11.16	(El Harmoudi et al., 2014)
CB-C carbon black	68.60	(Kuśmierek et al., 2016)
CB-V carbon black	72.20	(Kuśmierek et al., 2016)
Nano-sized Rice Husk (n-RH)	76.92	(Evy and Chidambaram, 2016)
Biochar from Switchgrass (*Panicumvirgatum*)	133.00	(Essandoh et al., 2017)
Carbon Nanotubes (CNTs)	83.33	(Hue et al., 2018)
LDH [Co–Al–Cl]	27.174	(This study)

$$\Delta G^{\circ} = -RTlnK_c \tag{8}$$

$$lnK_c = \frac{-\Delta H}{R}\frac{1}{T} + \frac{\Delta S^{\circ}}{R} \tag{9}$$

$$K_C = K_F\,\rho\left(\frac{10^6}{\rho}\right)^{\left(1-\frac{1}{n}\right)} \tag{10}$$

where ρ is the density of pure water (assumption on 1.0 g mL^{-1}), R is the gas constant (8.314 J K^{-1} mol^{-1}), T the temperature in K and K_c is the equilibrium constant (L mg^{-1})

The slope and intercept of the Van't Hoff plot is equal to $-\Delta H^{\circ}/R$ and $\Delta S^{\circ}/R$, respectively. Thermodynamic parameters obtained are summarized in Fig. 8.

The heat of adsorption ΔH for the sorption of 2,4-D onto [Co–Al–Cl] LDH can be calculated from the temperature dependence of the equilibrium adsorption constant, K. A plot of ln K_c *vs.*1/T (Fig. 8), should be linear with slope $-\Delta H^{\circ}/R$ and intercept $\Delta S^{\circ}/R$. ΔH° was found to be - 51.2 kJ mol^{-1} while ΔS° was - 126.6 J K^{-1} mol^{-1}.

The ΔG° values (obtained from Eq. (9) using equilibrium constant (K_c) derived from the Freundlich constant (K_F) (Tran et al., 2016) at different temperatures are negative and decrease with an increase in the temperature, revealing an adsorption process more effective under raised temperatures. The ΔH° value of - 51.2 kJ mol^{-1}, lower than the value of - 40 kJ mol^{-1}, indicated the exothermic process and predominance of physical adsorption. Besides, the low value of ΔH° implies that there was loose bonding between the adsorbate molecules and the adsorbent surface (Singh, 2000). Then, activation energy for physisorption is also very low and hence it is practically a reversible process. The ΔS° value of - 126.6 J K^{-1} mol^{-1} suggesting a decrease in the degree of freedom of the adsorbed species (Dogan et al., 2006).

3.7. Characterization of the [Co–Al–Cl] LDH before and after 2,4-D adsorption

The FT-IR spectra of [Co–Al–Cl] LDH, before and after 2,4-D adsorption, are shown in Fig. 9.

The broad strong absorption band at region from 3671 to 3087 cm^{-1} is attributed to the stretching vibrations of surface and interlayer water molecules and hydroxyl groups (Wei et al., 2006). This is related to the formation of hydrogen bonds of interlayer water with guest anions as well as with hydroxide groups of layers. The weaker band at 1623 cm^{-1} is due to the bending mode of water molecules and the bands centered at 540 and 420 cm^{-1} are attributed to M-O-H and O-M-O lattice vibrations, respectively (Li et al., 2004; Nejati and Rezvani, 2012). In the FT-IR spectrum of 2,4-D (shown in Fig. 9 (a)) absorption band at 1477 cm^{-1}

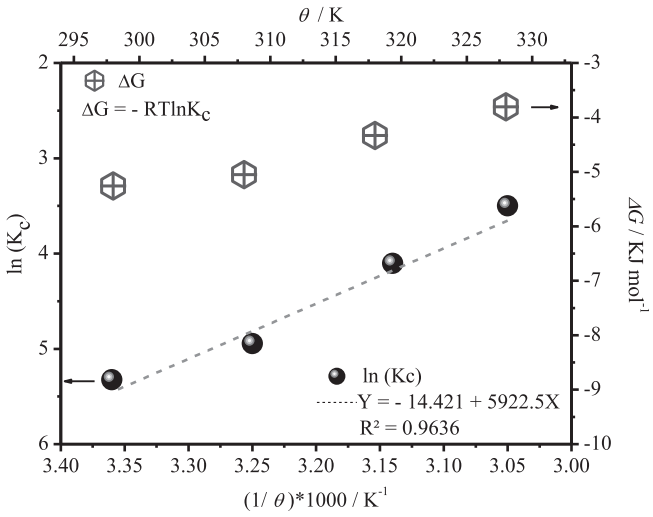

Fig. 8. Variation of K_C and ΔG as a function of temperature for 2,4-D adsorption by the [Co–Al–Cl] LDH.

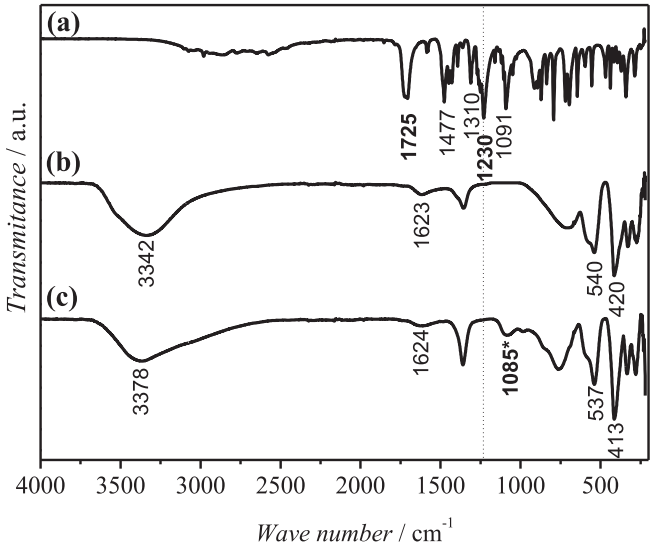

Fig. 9. FT-IR spectra of: (a) 2,4-D; (b) [Co–Al–Cl] LDH before 2,4-D adsorption and (c) [Co–Al–Cl] LDH after 2,4-D adsorption.

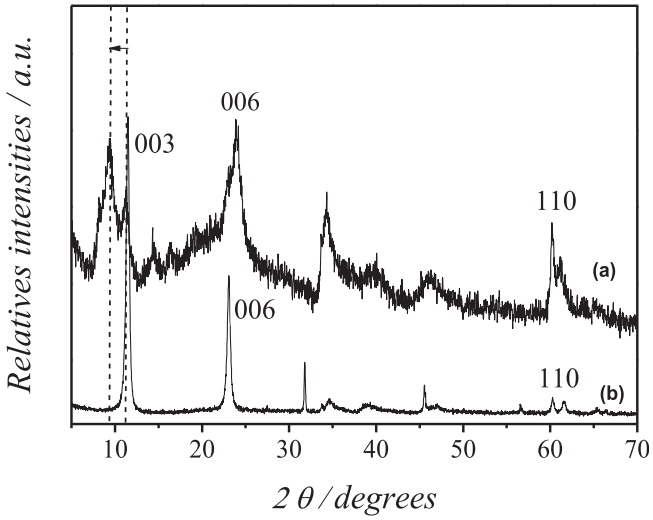

Fig. 10. X-ray patterns of: (a) [Co–Al–Cl] HDL before 2,4-D adsorption and (b) [Co–Al–Cl] HDL after 2,4-D adsorption.

Table 7
Unit cell parameters for [Co–Al–Cl] LDH before and after adsorption.

Sample	d_{003}-value/Å	a*/Å	c**/Å	V ***/Å^3	Representation of the unit cell
Hydrotalcite JCPDS 14-191	7.7433	3.0700	23.2300	189.60	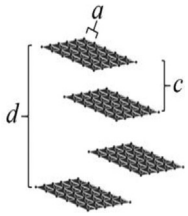
[Co–Al–Cl] LDH **before** adsoption	7.7100	3.0704	23.1300	188.92	
[Co–Al–Cl] LDH **after** adsoption	7.8635	3.0769	23.5905	193.43	

(*) a = 2 x d110; (**) c = 3 x d003; (***) V = volume.

(*) a = 2 x d110; (**)c = 3 x d003; (***).$V = \frac{\sqrt{3}\,a^2c}{2} = 0.866a^2c$.

corresponds to the C=C vibration of the aromatic ring. The two other bands centered at 1310 cm^{-1} and 1091 cm^{-1} cause by the antisymmetric and symmetric vibrations of C–O–C, respectively. On the other hand, absorption bands centered at 1725 cm^{-1} and 1230 cm^{-1} are attributed to the stretching vibrations of the C=O and O–H deformation coupled with C–O groups, respectively (Pavlovic et al., 2005). The FT-IR spectrum of LDH after adsorption of 2,4-D (shown in Fig. 9 (c)) indicated the 2,4-D related bands present in conjunction with those of LDH. In 2,4-D adsorbed on LDH, the two bands at 1725 and 1230 cm^{-1}, have disappeared and new band of the 2,4-D has appeared at 1085 cm^{-1} which indicates symmetric vibrations of 2,4-D.

The X-ray diffractogram of the [Co–Al–Cl] LDH before adsorption showed well-defined diffraction peaks, which were indexed to JCPDS 14-191 card Fig. 10 (a). In the X-ray diffractogram of [Co–Al–Cl] LDH after adsorption (Fig. 10 (b)) there is a shift of the value of 2θ to lower values when compared to that obtained for [Co–Al–Cl] LDH. This displacement of plane (003) corresponds to an increase in the interlamellar distance d_{003} (Arai and Ogawa; 2009) due to the intercalation of 2,4-D in the interlayer structure of the [Co–Al–Cl] LDH.

Table 7 shows the unit cell parameters of hydrotalcite and of the [Co–Al–Cl] LDH before and after 2,4-D adsorption.

It was observed, from the d_{003} value calculated after adsorption, an increase from 7.7100 to 7.8635 Å and consequently there was also an increase in the unit cell volume, as verified in Table 7. The d_{003}-value of 7.71 Å is typical of intercalated hydrated chloride ions (Leroux et al., 2004).

4. Conclusions

From the present study, it can be seen that [Co–Al–Cl] LDH, commonly used as electrodes in supercapacitors, was synthesized by the co-precipitation method at constant pH and tested as adsorbent for the removal of 2,4-D from contaminated waters. This LDH presented mesoporosity, suitable specific surface area and good adsorption affinity toward pesticide 2,4-D. Whereas adsorption is a simple and low-cost method for removal of 2,4-D from aqueous solutions, here, this process was relatively fast because the adsorption equilibrium was reached after 60 min, occurring mainly in the first minutes of contact. A very good agreement with experimental data in the case of the kinetic model of pseudo-second order (R^2 = 0.9998 for 2,4-D 60 mg L^{-1} adsorption). The intra-particle diffusion model was not the sole rate-controlling factor, indicating that the adsorption of 2,4-D by the [Co–Al–Cl] LDH is a complex process, involving both boundary layer and intra-particle diffusion, corroborated by FT-IR and X-ray data, respectively. Thermodynamic study signified that the adsorption reaction was spontaneous and exothermic. However, the negative standard entropy change (ΔS°) suggested a decrease in the degree of freedom of the adsorbed species. The adsorption of 2,4-D pesticide on [Co Al Cl] LDH has been described by the Freundlech isotherm, predominating the physical adsorption. The increase in the interlamellar distance (d_{003}) indicated an intercalation of 2,4-D in the interlayer structure of the [Co–Al–Cl] LDH. Thus, [Co–Al–Cl] LDH can be effectively used as an adsorbent for the removal of 2,4-D from contaminated waters.

Declarations

Author contribution statement

Canobre Sheila: Analyzed and interpreted the data; Contributed reagents, materials, analysis tools or data; Wrote the paper.

Josiane Calisto: Performed the experiments; Analyzed and interpreted the data; Wrote the paper.

Leonardo Freitas: Conceived and designed the experiments; Performed the experiments; Analyzed and interpreted the data.

Ingrid Pacheco: Performed the experiments; Analyzed and interpreted the data.

Laiane Santana: Conceived and designed the experiments; Analyzed and interpreted the data.

Wélique Fagundes: Analyzed and interpreted the data.

Amaral Fabio: Contributed reagents, materials, analysis tools or data; Wrote the paper.

Funding statement

This work was supported by FAPEMIG [grant numbers: APQ-02249-14 and APQ-03219-14], CNPq, CAPES and Rede Mineira de Química.

Competing interest statement

The authors declare no conflict of interest.

Additional information

No additional information is available for this paper.

References

Arai, Y., Ogawa, M., 2009. Preparation of Co–Al layered double hydroxides by the hydrothermal urea method for controlled particle size. Appl. Clay Sci. 42 (3-4), 601–604.

Aumeier, B.M., Dang, A.H.Q., Ohs, B., Yüce, S., Wessling, M., 2019. Aqueous-phase temperature swing adsorption for pesticide removal. Environ. Sci. Technol. 53, 919–927.

Bernardo, M.P., Moreira, F.K.V., Colnago, L.A., Ribeiro, C., 2016. Physico-chemical assessment of [Mg-Al-PO_4]-LDHs obtained by structural reconstruction in high concentration of phosphate. Colloids Surf., A 497, 53–62.

Białas, A., Mazur, M., Natkanski, P., Dudeka, B., Kozak, M., Wacha, A., Kustrowski, P., 2016. Hydrotalcite-derived cobalt–aluminummixed oxide catalysts for toluene combustion. Appl. Surf. Sci. 362, 297–303.

Boyd, W.J., Adamson, A.W., Myers, L.S., 1947. The exchange adsorption of ions from aqueous solutions by organic zeolites, II. Kinetics. J. Am. Chem. Soc. 69, 2836–2848.

Carter, A.D., 2000. Herbicide movement in soils: principles, pathways and processes. Weed Res. 40, 113–122.

Feng, C.Y., Chen, P.C, Li, W.S., 2008. Adsorption of 2,4-D on Mg/Al–NO_3 layered double hydroxides with varying layer charge density. Appl. Clay Sci. 40, 193–200.
Crepaldi, E.L., Pavan, P.C., Valim, J.B., 2000. Comparative study of the coprecipitation methods for the preparation of Layered Double Hydroxides. J. Braz. Chem. Soc. 11, 64–70.
Crepaldi, E.L., Valim, J.B., 1998. Layered double hydroxides: structure, synthesis, properties and applications. Quim. Nova 21, 300–311.
Dogan, M., Alkan, M., Demirbas, O., Ozdemir, Y., Ozmetin, C., 2006. Adsorption kinetics of maxilon blue GRL onto sepiolite from aqueous solutions. Chem. Eng. J. 124, 89–101.
El Harmoudi, H., El Gaini, L., Daoudi, E., Rhazi, M., Boughaleb, Y., El Mhammedi, Migalska-Zalas, A., Bakasse, M., 2014. Removal of 2,4-D from aqueous solutions by adsorption processes using two biopolymers: chitin and chitosan and their optical properties. Opt. Mater. 36, 1471–1477.
Essandoh, M., Wolgemuth, D., Pittman Jr., C.U., Mohan, D., Mlsna, T., 2017. Phenoxy herbicide removal from aqueous solutions using fast pyrolysis switchgrassbiochar. Chemosphere 174, 49–57.
Evy, A.A.M., Chidambaram, R., 2016. Rice husk as a low cost nanosorbent for 2,4-dichlorophenoxyacetic acid removal from aqueous solutions. Ecol. Eng. 92, 97–105.
Feigenbrugel, V., Le Calvé, S., Mirabel, P., 2006. Molar absorptivities of 2,4 - D ,cymoxanil, fenpropidin, isoproturon and pyrimethanil in aqueous solution in the near-UV. Spectrochim. Acta A. 63, 103–110.
Freundlich, H.M., 1906. Over the adsorption in solution. J. Phys. Chem. 57, 385–470.
Fytianos, K., Voudrias, E., Kokkalis, E., 2000. Sorption–desorption behavior of 2,4-dichlorophenol by marine sediments. Chemosphere 40, 3–6.
Ghemit, R., Boutahala, M., Kahoul, A., 2017. Removal of diclofenac from water with calcined ZnAlFe-CO_3 layered double hydroxides: effect of contact time, concentration, pH and temperature. Desalin. Water Treat. 83, 75–85.
Gregg, S.J., Sing, K.S.W. (Eds.), 1982. Adsorption, Surface Area and Porosity. Academic Press, London.
Gao, J., Xuan, H., Xu, Y., Liang, T., Han, X., Yang, J., Han, P., Wang, D., Du, Y., 2018. Interconnected network of zinc-cobalt layered double hydroxide stick onto rGO/nickel foam for high performance asymmetric supercapacitors. Electrochim. Acta 286, 92–102.
Haddad, M., Oie, C., Duy, S.V., Sauvé, S., Barbeau, B., 2019. Adsorption of micropollutants present in surface waters onto polymeric resins: impact of resin type and water matrix on performance. Sci. Total Environ. 660, 1449–1458.
Hamilton, D.J., Ambrus, A., Dieterle, R.M., Felsot, A.S., Harris, C.A., Holland, P.T., Katayama, A., Kurihara, N., Linders, J., Unsworth, J., Wong, S.S., 2003. Regulatory limits for pesticide residues in water. Pure Appl. Chem. 75, 1123–1155.
Hue, H.K., Anh, L.V., Thiep, T.V., 2018. Study of the adsorption of 2,4-dichlorophenoxyacetic acid from the aqueous solution onto carbon nanotubes. Viet. J. Chem. 56, 191–196.
Khoei, A.J., Joogh, N.J.G., Darvishi, P., Rezaei, K., 2019. Application of physical and biological methods to remove heavy metal, arsenic and pesticides, malathion and diazinon from water. Turk. J. Fish. Aquat. Sci. 19, 21–28.
Kinniburgh, D.G., 1986. General purpose adsorption isotherms. Environ. Sci. Technol. 20 (9), 895–904.
Kuśmierek, K., Szala, M., Świątkowski, A., 2016. Adsorption of 2, 4-dichlorophenol and 2, 4-dichlorophenoxyacetic acid from aqueous solutions on carbonaceous materials obtained by combustion synthesis. J. Taiw. Inst. Chem. Eng. 63, 371–378.
Lai, F., Huang, Y., Miao, Y., Liu, T., 2015. Controllable preparation of multi-dimensional hybrid materials of nickel-cobalt layered double hydroxide nanorods/nanosheets on electrospun carbon nanofibers for high-performance supercapacitors. Electrochim. Acta 74, 456–463.
Langmuir, I., 1918. The adsorption of gases on plane surfaces of glass, mica and platinum. J. Am. Chem. Soc. 40, 1361–1403.
Leroux, F., Gachon, J., Besse, J.P., 2004. Biopolymer immobilization during the crystalline growth of layered double hydroxide. J. Solid State Chem. 177, 245–250.
Li, C., Wang, G., Evans, D.G., Duan, X., 2004. Incorporation of rare-earth ions in Mg–Al layered double hydroxides: intercalation with an [Eu(EDTA)]− chelate. J. Solid State Chem. 177, 4569–4575.
Li, M., Yuan, P.W., Guo, S.H., Liu, F., Cheng, J.P., 2017a. Design and synthesis of Ni-Co and Ni-Mn layered double hydroxides hollow microspheres for supercapacitor. Int. J. Hydrogen Energy 42, 28797–28806.
Li, Q., Sun, J., Ren, T., Guo, L., Yang, Z., Yang, Q., Chen, H., 2017b. Adsorption mechanism of 2, 4-dichlorophenoxyacetic acid onto nitric-acid-modified activated carbon fiber. Environ. Technol. 39, 895–906.
Mostafa, M.S., Mohamed, N.H., 2016. Towards novel adsorptive nanomaterials: synthesis of Co^{2+} Mo^{6+} LDH for sulfur and aromatic removal from crude petrolatum. Egypt. J. Petrol. 25, 221–227.
Nejati, K., Rezvani, Z., 2012. Synthesis and characterization of nanohybrids of olsalazine-intercalated Al–Mg layered double hydroxide. J. Exp. Nanosci. 7, 412–425.
Nejati, K., Davary, S., Saati, M., 2013. Study of 2,4 - D removal by Cu-Fe-layered double hydroxide from aqueous solution. Appl. Surf. Sci. 280, 67–73.
Newman, S.P., Jones, W., 1998. Synthesis, characterization and applications of layered double hydroxides containing organic guests. New J. Chem. 22, 105–115.
Pavlovic, I., Barriga, C., Hermosín, M.C., Cornejo, J., Ulibarri, M.A., 2005. Adsorption of acidic pesticides 2,4-D, Clopyralid and Picloram on calcined hydrotalcite. Appl. Clay Sci. 30, 125–133.
Pavlovic, I., González, M.A., Rodríguez-Rivas, F., Ulibarri, M.A., Barriga, C., 2013. Caprylate intercalated layered double hydroxide as adsorbent of the linuron, 2,4 - D B and metamitron pesticides from aqueous solution. Appl. Clay Sci. 80, 76–84.
Pourfarzad, H., Shabani-Nooshabadi, M., Ganjali, M.R., Kashani, H., 2019. Synthesis of Ni–Co-Fe layered double hydroxide and Fe_2O_3/Graphene nanocomposites as actively materials for high electrochemical performance supercapacitors. Electrochim. Acta 317, 83–92.
Qiu, J., Villemure, G., 1997. Anionic clay modified electrodes: electron transfer mediated by electroactive nickel, cobalt or manganese sites in layered double hydroxide films. J. Electroanal. Chem. 428, 165–172.
Regalbuto, J.R., Robles, J., 2004. The engineering of Pt/Carbon Catalyst Preparation. University of Illinois, Chicago. http://www.scielo.br/scielo.php?script=sci_nlinks&ref=000174&pid=S0100-40422006000600001500019&lng=en.
Salman, J.M., Hameed, B.H., 2010. Adsorption of 2, 4-dichlorophenoxyacetic acid and carbofuran pesticides onto granular activated carbon. Desalination 256, 129–135.
Shujun, Y., Yang, L., Yuejie, A., Xiangxue, W., Rui, Z., Zhongshan, C., Zhe, C., Guixia, Z., Xiangke, W., 2018. Rational Design ofcarbonaceousnanofiber/Ni-Allayereddouble Hydroxide nanocomposites for high-efficiency removal of heavy metals from aqueous solutions. Enviro 242, 1–11.
Singh, D., 2000. Studies of the adsorption thermodynamics of oxamyl on fly ash adsorp. Sci. Technol. 18, 741–748.
Tran, H.N., You, S.-J., Chao, H.-P., 2016. Thermodynamic parameters of cadmium adsorption onto orange peel calculated from various methods: a comparison study. J. Environ. Chem. Eng. 4 (3), 2671–2682.
Tsai, W.T., Hsien, K.J., Chang, Y.M., Lo, C.C., 2005. Removal of herbicide paraquat from an aqueous solution by adsorption onto spent and treated diatomaceous earth. Bioresour. Technol. 96 (6), 657–663.
Weber, W.J., Morris, J.C., 1963. Kinetics of adsorption on carbon from solution. J. Sanit. Eng. Div. 89, 31–60.
Wei, M., Xu, X., He, J., Yuan, Q., Rao, G., Evans, D.G., Pu, M., Yang, L., 2006. Preparation and thermal decomposition studies of l-tyrosine intercalated MgAl, NiAl and ZnAl layered double hydroxides. J. Phys. Chem. Solids 67, 1469–1476.
WHO, 2003. 2,4-D in drinking-water. Background document for preparation of WHO guideline for drinking-water quality. WHO/SDE/WSH/03.04/70. World Health Organization, Geneva.
Ye, N., Cimetiere, N., Heim, V., Fauchon, N., Feliers, C., Wolbert, D., 2019. Upscaling fixed bed adsorption behaviors towards emerging micropollutants in treated natural waters with aging activated carbon: model development and validation. Water Res. 148, 30–40.
Yu, S., Liu, Y., Ai, Y., Wang, X., Zhang, R., Chen, Z., Chen, Z., Zhao, G., Wang, X., 2018. Rational design of carbonaceous nanofiber/Ni-Al layered double hydroxide nanocomposites for high-efficiency removal of heavy metals from aqueous solutions. Environ. Pollut. 242, 1–11.
Yu, S., Wang, J., Song, S., Sun, K., Li, J., Wang, X., Chen, Z., Wang, X., 2017. One-pot synthesis of graphene oxide and Ni-Al layered double hydroxides nanocomposites for the efficient removal of U(VI) from wastewater. Sci. China Chem. 60, 415–422.
Zhang, B., Yuan, S., Sun, D., Li, Y., Wu, T., 2018. Experimental and theoretical calculation investigation of 2,4-dichlorophenoxyacetic acid adsorption onto core-shell carbon microspheres@layered double hydroxide composites. RSC Adv. 8, 856–866.
Zhao, G., Chen, X., Zou, J., Li, C., Liu, L., Zhang, T., Yu, J., Jiao, F., 2018. Activation of peroxymonosulfate by Fe_3O_4-CsxWO_3/NiAl layered double hydroxide composites for the degradation of 2,4-dichlorophenoxyacetic acid. Ind. Eng. Chem. Res. 57, 16308–16317.